Journal of Applied Mechanical Engineering
ISSN: 2168-9873

Huang et al., J Appl Mech Eng 2014, 3:1
DOI: 10.4172/2168-9873.1000135

Research Article Open Access

A Nanocomposite Approach: Lowering Thermal Conductivity of Si-Ge Thermoelectric Materials for Power Generation Applications

Dale Huang[1], Bao Yang[1]* and Thanh Tran[2]

[1]Department of Mechanical Engineering, University of Maryland, College Park, MD 20742
[2]Naval Surface Warfare Center, Carderock Division, West Bethesda, MD 20817-5700

Abstract

Solid-state thermoelectric power generation devices have many attractive features compared with other methods of power generation, such as long life, no moving parts, no emissions of toxic gases, light weight, low maintenance, and high reliability. The first part of this paper discusses the basic thermoelectric effects and their underlying physics, and the second part introduces nanostructured thermoelectric materials and their characteristics. Especially, the synthesis and characterization of two-component Si-Genanocomposites have been discussed in details. This nanostructured approach is easily scalable and can be used to enhance the dimensionless figure-of-merit ZT of thermoelectric materials resulting in a more efficient thermoelectric devices.

Keywords: Thermal Conductivity; Thermoelectric materials; Thermoelectric Power Generators

Introduction

Solid-state thermoelectric power generation devices have many attractive features compared with other methods of power generation, such as long life, no moving parts, no emissions of toxic gases, light weight, low maintenance, and high reliability [1-3]. Thermoelectric power generators have found direct applications in areas as diverse as national security (portable power for remote sensors and transmission devices in nuclear or other dangerous sites) [4], space exploration (power sources for spacecraft) [5-7], and health care (power sources for artificial organs) [8,9]. One tested and verified example is that NASA's Voyager 1 spacecraft, powered by radioactive thermoelectric generators, has travelled for 36 years and now is venturing into interstellar space.

In this paper, the fundamentals of thermoelectric technology will be discussed first. The second part of this paper is devoted to nanostructured thermoelectric materials, with focus on Si-Ge two-component nanocomposites, for power generation applications. It should be noted that the selection of the coverage is influenced by the research focus of the present authors and reflects their assessment of the field.

Fundamentals of thermoelectric technology

Thermoelectric Effects: Thermoelectric power generation is the direction conversion of heat (temperature differences) into electrical energy, using a phenomenon called the "Seebeck effect". There exist three basic thermoelectric effects: the Seebeck effect, Peltier effect, and Thomson effect. These three effects describe thermodynamically reversible processes, in which no entropy is generated. Other inevitable effects in thermoelectric process include Joule heating and thermal conduction, which lower the performance of thermoelectric devices to less than the thermodynamic limit, i.e., Carnot efficiency.

Seebeck Effect: The Seebeck effect describes the phenomenon of voltage generation when a material is subject to a temperature gradient under the open circuit condition. This effect was discovered by the Estonian physicist Thomas Johann Seebeckin 1821 [10]. The Seebeck effect is the principle at work behind thermoelectric power generation which converts temperature difference to electricity.

An applied temperature gradient causes charged carriers (electrons or holes) to diffuse from the hot to cold side in the material, as shown in Figure 1a. At the steady state, the internal field (Seebeck voltage), ΔV, generated from the difference in charged carrier concentration, balances the driven force for thermal diffusion. The absolute Seebeck coefficient for an individual material is defined as

$$S = -\frac{\Delta V}{\Delta T}, \quad (1)$$

where ΔV and ΔT are the voltage and temperature difference between the hot and cold sides of the material, respectively. The Seebeck coefficient has a unit of V, but microvolt per Kelvin ($\mu V/K$)

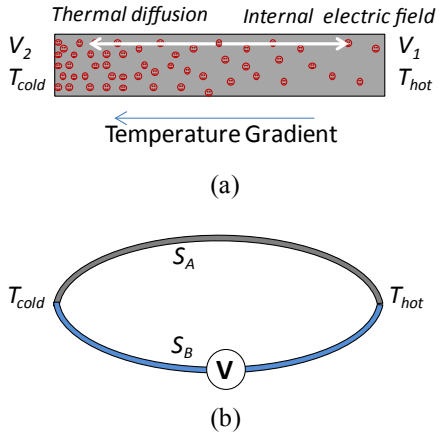

Figure 1: Seebeck effect in a single material (a) and a circuit consisting of two different materials A and B (b) [13].

***Corresponding author:** Bao Yang, Department of Mechanical Engineering, University of Maryland, College Park, MD 20742,Tel: 301-405-6007; E-mail: baoyang@umd.edu

Received November 21, 2013; **Accepted** December 26, 2013; **Published** January 06, 2014

Citation: Huang D, Yang B, Tran T (2014) A Nanocomposite Approach: Lowering Thermal Conductivity of Si-Ge Thermoelectric Materials for Power Generation Applications. J Appl Mech Eng 3: 135. doi:10.4172/2168-9873.1000135

is often used for thermoelectric materials. The Seebeck coefficient is sometimes called the thermal electromotive force (emf) coefficient or thermoelectric power [11].

A voltage can be established between two junctions as shown in Figure 1a of two different materials A and B if there is a temperature difference between them, as shown in Figure 1b. This configuration is a basic thermocouple. The Seebeck coefficient of the A-B couple is determined by

$$(S_A - S_B) = \frac{\Delta V}{\Delta T} \tag{2}$$

Equation (2) provides a way to determine an unknown Seebeck coefficient from a known one. The absence of Seebeck effect for superconductors has also made it possible to define an absolute Seebeck coefficient for individual materials.

In semiconductor materials, the Seebeck coefficient varies with doping. The n-type semiconductors have negative Seebeck coefficient while the p-type ones are positive. The magnitude of the Seebeck coefficient can be very large in semiconductors, e.g., larger than 200 microvolt per Kelvin in Bi_2Te_3 based alloys [11-13], due to their excessive electrons or holes generated by doping.

Peltier Effect: The Peltier effect is directly related to thermoelectric cooling devices, which is the reverse of the Seebeck effect [14]. The Peltier effect measures the amount of heat carried by electrical carriers (electrons or holes), the amount of heat moved is proportional to the current that flows. As shown in Figure 2a, the Peltier heat enters from one end of the material and is released at the other end. The absolute Peltier coefficient of a material defines the relationship between the heat power Q and the electric current I flow in the material, it can be expressed by the following equation

$$\Pi = \frac{Q}{I}, \tag{3}$$

where Π is the absolute Peltier coefficient of an individual material.

If the power is supplied to the circuit as shown in the above Figure 2b, the electric current must be continuous across the junctions; then heat is absorbed at one junction and generated at the other junction. The imbalance of the heat in and out at each junction creates cooling or heating effects. The Peltier heat Q absorbed at the junction is equal to

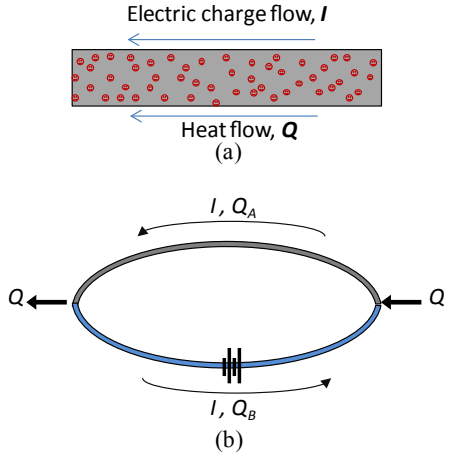

Figure 2: Peltier effect in a single material (a) and a circuit consisting of two different materials A and B (b) [13].

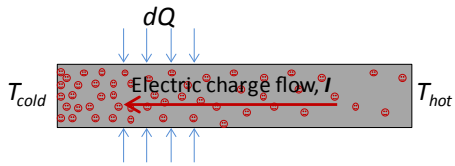

Figure 3: Thomson effect in a single material [13].

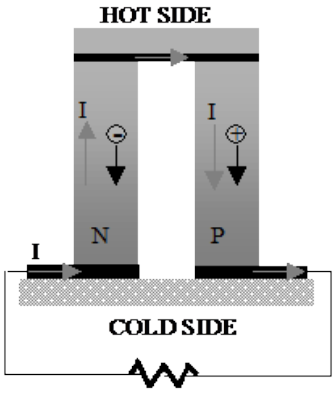

Figure 4: Schematic illustrate of thermoelectric elements operating in power generation modes.

$$Q = \Pi_{AB} I = (\Pi_A - \Pi_B) I \tag{4}$$

where I is the electric current, Π_{AB} is the Peltier coefficient of the junction between the materials A and B, and Π_A and Π_B are the absolute Peltier coefficient of the materials A and B, respectively.

Thomson Effect: The Thomson effect describes the heating or cooling phenomenon along a material which an electric current is passing through and is subject to a temperature gradient, as shown in Figure 3. This effect was discovered by Thomson (Lord Kelvin) in 1851 [15]. The Thomson coefficient τ is defined as

$$\frac{dQ}{dx} = \tau I \frac{dT}{dx} \tag{5}$$

Where dQ/dx is the rate of the heating per unit length, I is the electric current, and dT/dx is the temperature gradient applied to the material. The direction of heat flow dQ is determined by the choice of materials, the direction of the electric current, and the temperature gradient. The Thomson coefficient τ can be positive, negative, or zero.

Kelvin Relation: The aforementioned three thermoelectric effects are due to flow of electrons or holes and their interaction with the lattice and thus these thermoelectric coefficients are interrelated. Thomson (Lord Kelvin) found relationships between the three coefficients in 1854, implying that only one could be considered unique [16].

The first Kelvin relation gives relation between the Thomson coefficient and the temperature derivative of the Seebeck coefficient,

$$\tau = T \frac{dS}{dT}, \tag{6}$$

where T is the absolute temperature in Kelvin, τ is the Thomson coefficient, and S is the Seebeck coefficient. The second Kelvin relation is

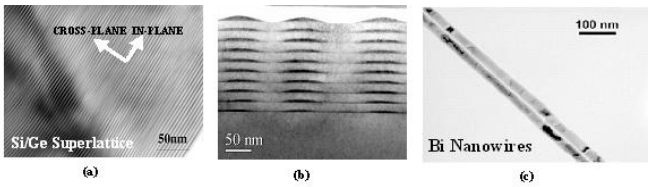

Figure 5: Examples of nanostructures for potential thermoelectric applications: (a) Si/Gesuperlattices, (b) quantum-dot Si/Gesuperlattices, and (c) quantum wires [43].

$$\Pi = ST \ , \tag{7}$$

where Π is the Peltier coefficient. These two equations provide a fundamental link between thermoelectric cooling and power generation. The Kelvin relations can be derived rigorously using irreversible thermodynamics.

Joule Heating and Heat Conduction: Joule heating and heat conduction are two irreversible processes that lower the performance of thermoelectric devices to less than the thermodynamic limit, i.e., Carnot efficiency. The Joule heating Q is given by

$$Q = I^2 R \ , \tag{8}$$

where I is the electric current and R is the electrical resistance. In thermoelectric generators, the internal resistance, i.e., Joule heating, will consume part of the generated electricity, therefore lowering the system efficiency.

The heat conduction for a material under a temperature gradient is given by

$$Q = -Ak\frac{dT}{dx} \ , \tag{9}$$

where A is the cross-section area of the material, k is its thermal conductivity, and dT/dx is the temperature gradient. In any material, a temperature gradient leads to an irreversible heat flow which opposes the temperature gradient. A good thermoelectric material must have a large Seebeck coefficient, a low electrical resistivity and a low thermal conductivity to reduce the effects of Joule heating and heat leakage by conduction.

Thermoelectric power generation devices

The schematic of a thermoelectric power generator is shown in Figure 4, which consists of a p-branch with a positive Seebeck coefficient and an n-branch with a negative Seebeck coefficient, as shown in Figure 4. These two branches are joined by an interconnecting metal which forms a low-resistivity ohmic contact. A thermoelectric device is typically made of multiple thermocouples that are connected such that the electric current flow is in series while the heat flow is in parallel. The reason for the use of both p and n branches is because their Seebeck and Peltier coefficients are of opposite sign, such that both branches contribute to the desired thermoelectric effect. These branches are connected electrically in series and thermally in parallel. In this thermoelectric generator, the electrons and holes at the hot side have higher thermal velocity but lower density, and the diffusion will be balanced by the built-in electro motive force (emf). The built-in emf may drive an external load.

The energy conversion efficiency of a thermoelectric power generator is determined by both the operational temperature and the figure-of-merit of thermoelectric materials,

$$\eta = \frac{T_H - T_C}{T_H} \times \frac{((1+ZT)^{0.5} - 1)}{(1+ZT)^{0.5} + T_C / T_H} \tag{10}$$

where η is the energy conversion efficiency, ZT is the dimensionless figure-of-merit, T_H and T_C are the temperatures at the hot and cold ends of thermoelectric legs, respectively and T is the average temperature of T_H and T_C. The dimensionless figure-of-merit for a single material is given by [11].

$$Z = \frac{S^2}{k\rho} \ . \tag{11}$$

This figure-of-merit Z is a measure of the material's potential for making an efficient thermoelectric device. It includes electrical resistivity ρ due to Joule heating. It has thermal conductivity k in its denominator because of the heat leakage from the hot to cold side through conduction. The figure of merit Z has a unit of inverse Kelvin. The dimensionless form ZT, a product of Z and absolute temperature T, is commonly used in device analysis. From a microscopic point of view, the figure of merit is influenced by charge and heat transport as well as their coupling in thermoelectric materials. The best ZT materials are found in heavily doped semiconductors. The commercially available bulk Bismuth Telluride Bi_2Te_3 alloy has a ZT of 1 around room temperature [11].

Nanostructured Thermoelectric Materials

State of the art thermoelectric nanomaterials

The use of nanostructures for thermoelectric applications was triggered by the conceptual studies in the early 1990s that identified the potential benefits of quantum confinement of electrons and phonons and phonon interface scattering [17-21]. Since then, much attention has been paid to the development of nanostructures for enhancing ZT [22-42]. Figure 5 shows some samples of nanostructures currently under study.

The prediction of ZT enhancement in low dimensional materials has been experimentally demonstrated in Bi_2Te_3/Sb_2Te_3 superlattices [32] and PbSeTe/PbT [34] quantum-dot superlattices. Bi_2Te_3/Sb_2Te_3 superlattices were reported to have a ZT~2.5 around room temperature, the highest ZT to date, and PbSeTe/PbTe quantum-dot superlattices exhibit a ZT of ~2.0 at elevated temperature (about 500K). Recently, a

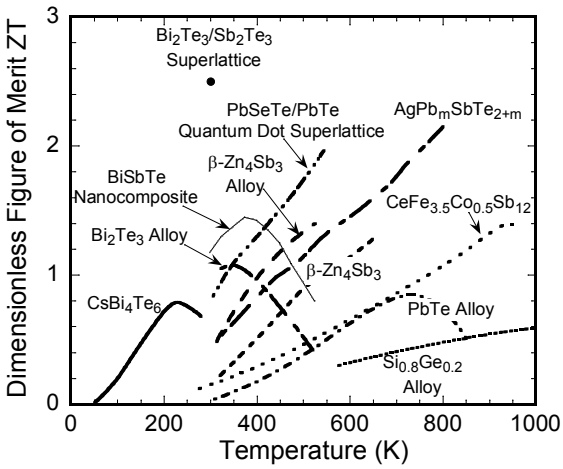

Figure 6: ZT of state-of-the-art thermoelectric materials [13].

significant ZT increase has been reported in bulk materials made from nanocrystalline powders of p-type BiSbTe, reaching a peak ZT of 1.4 at 100°C [42]. This nanocomposite fabrication method is cost effective and can be scaled up for mass production. Figure 6 is the snapshot of state-of-the-art thermoelectric materials, including both bulk and nanostructured materials [43].

Exploring two-component nanocomposites

Silicon-Germanium alloys have been the primary thermoelectric materials in power generation devices for operation at the temperature above 600°C [44], having long been used in radio-isotope Thermoelectric Generators (RTGs) for deep space missions to convert radio-isotope heat into electricity [44]. SiGe also holds promise in terrestrial applications such as waste heat recovery [45]. The performance of these materials depends on the dimensionless figure-of-merit ZT [44]. In order to achieve high ZT values, materials must possess a unique combination of electrical and thermal transport properties: low metal-like resistivity, high insulator-like Seebeck coefficient, and low glass-like thermal conductivity [44]. Materials with a large thermoelectric figure of merit can be used to develop efficient solid-state devices that convert heat into electricity. Lowering thermal conductivity of thermoelectric materials represents one approach for a higher thermoelectric figure-of-merit.

Therefore, the focus of this silicon germanium materials study is to lower the thermal conductivity by using a nanostructured nanocomposite approach. The original concept is for either nanoparticles embedded in a host or hetero structure geometry with nanoparticles of different materials adjacent to each other, so-called two-component nanocomposites. For the hetero structure geometry, when the two materials are the same, the nanocomposite is essentially a material with nanometer sized grains [46]. Because these nanostructures have a size smaller than the phonon mean free path, but greater than the electron or hole mean free path, phonons are more strongly scattered by the interfaces than are electrons or holes, resulting in a net increase in ZT [46].

Samples Preparation: The samples were prepared by high energy planetary ball milling of pure Si and pure Ge crystals from Sigma-Aldrich. Stoichiometric amounts of the respective powders, i.e., atomic ration of Si and Ge is 8 to 2, were weighed out in an argon-filled glove box and loaded into a zirconium oxide vial which was sealed and subsequently loaded into a customized Retsch PM100 planetary ball mill (Haan, Germany). After several hours of processing, the powders were isolated and dried under ultra pure nitrogen and then hot pressed using high density steel dies at temperatures in excess of (343°C). The hot pressed pellets were approximately 13.0 mm in diameter and 2.77 mm thick. The mass density of the pressed pellets was achieved close to within 1-2% of the theoretical bulk density of the stoichiometric composition of the powdered material.

Characterization of Microstructure and Thermal Conductivity: The fact that the nanoparticles easily aggregate, it is challenging to precisely determine their size distribution and chemical purity [47]. A combination of techniques is therefore useful to characterize the batches of nanoparticles and pellets. The scanning electron microscopy (SEM) images of the ball milled micro- and nano-scale silicon germanium nanocomposites are presented in Figure 7. The images shows nanoparticle agglomerates approximately (100 to 300) nm in diameter. Upon high-temperature compaction, SEM imaging of the hot pressed pellet surfaces (Figure 7) shows that the individual particles range in size 100-500 nm. The nanostructures are considerably dense

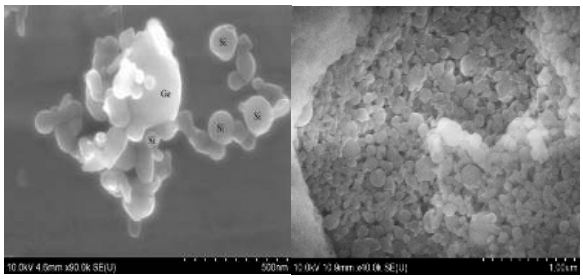

Figure 7: (Left) SEM Image of SiGeNanocomposite. (Right) SEM Image for the Surface of SiGe Pellet.

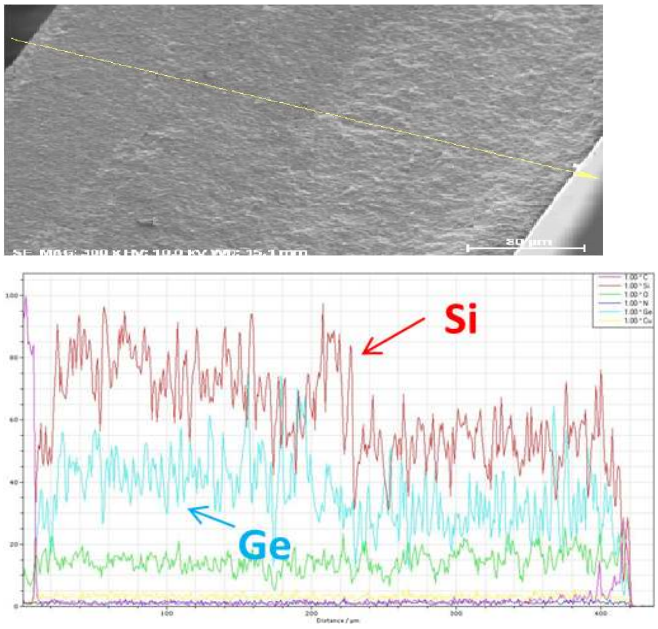

Figure 8: EDS Line Scan of Cross-Section of SiGe Nanocomposite Pellet.

with nano and submicron grains. Observation from the SEM data reveals a grain size distribution ranging from 100 to 800 nm in the Si-Ge two-component nanocompositefabricated using high energy ball mill and hot press.

The energy dispersive spectroscopy (EDS) was performed by line scan along the cross-section of the SiGe pellet. The total distance of the cross-section surface was measured to be approximately 400 μm Figure 8. The Intensity (atomic %) vs. Distance plot shows the composition of the sample runs consistently with the $Si_{0.8}Ge_{0.2}$ and also features higher percentages of silicon than germanium across the cross section of the thin disk.

Thermal conductivity of the Si-Genanocomposites was measured using the steady-state method also known as guarded hot plate techniques [13]. The bulk thermoelectric sample is typically in a form of a disk or plate with uniform cross section and a small thickness and placed in between an electric heater and heat sink. All the measurement of thermal conductivity follows the absolute method listed in ASTM C177-04 [48].

As shown in Figure 9, the developed nanocomposites demonstrated a lower thermal conductivity than the RTG (SiGe based TE material) module and the p-type nanostructured bulk SiGe alloys. Figure 9

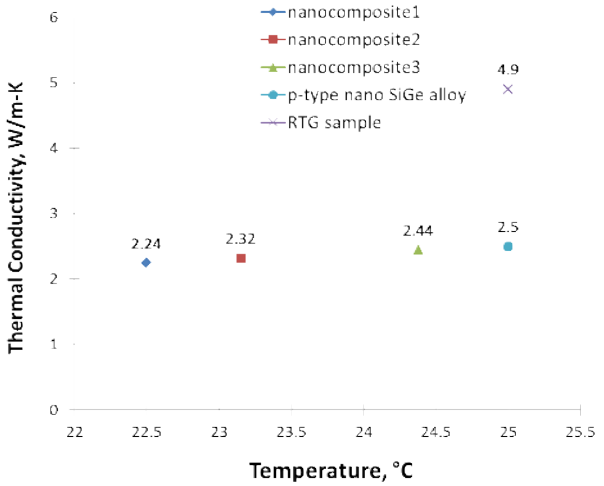

Figure 9: Thermal conductivity of three hot-pressed undoped $Si_{0.8}Ge_{0.2}$ nanocomposites (diamonds, squares, triangles), in comparison with p-type SiGe bulk samples used in RTGs for space power missions (crosses) and the p-type nanostructured bulk SiGe alloys (circles).

shows the thermal conductivity of undoped $Si_{0.8}Ge_{0.2}$, two-component nanocomposites (2.24, 2.32 and 2.44 W/m-K), is 50.2 to 54.3% lower than that of the RTG samples (4.9 W/m-K) and 2.4 to 10.4% lower than the p-type nanostructured bulk silicon germanium alloys (2.5 W/m-K) [45]. The significant reduction of the thermal conductivity in the nanostructured samples is mainly due to the increases phonon scattering at the heterogeneous interfaces of the nano composites [47].

Conclusion

The first part of this paper discusses the basic thermoelectric effects and their underlying physics, and the second part introduces nanostructured thermoelectric materials and their characteristics. Especially, the synthesis and characterization of two-component Si-Ge nanocomposites have been discussed in details. This nanostructured approach is easily scalable and can be used to enhance the dimensionless figure-of-merit ZT of thermoelectric materials resulting in more efficient thermoelectric devices. This approach is certainly a good and economical solution for low efficiency of existing thermoelectric materials, which are often used in automotive, industrial, waste heat recovery and space power generation applications.

Acknowledgements

This research is financially supported by NSF under Grant CBET1232949.

References

1. Nolas G, Sharp J, Goldsmid HJ (2001) Thermoelectrics: Basic Principles and New Materials Developments. Springer, Berlin, Germany.
2. Tritt TM (2001) Recent trend in thermoelectric materials research, in Semiconductor and Semimetals. Academic Press, San Diego, California.
3. Chen G (2004) "Nanostructures for thermoelectric energy conversion," in Heat Transfer and Fluid Flow in Microscale and Nanoscale Structures, BSM Faghri, Ed., Southampton: WIT Press 45-91.
4. Glenn GD (1986) A microprocessor-based controller for a thermoelectric generator, 32nd International Power Sources Symposium, Cherry Hill, NewJersey, USA.
5. Bass JC, Allen DT (1999) Milliwatt radioisotope power supply for space applications, 18th International Conference on Thermoelectrics, Baltimore, MD, USA.
6. Pustovalov A (1985) Certification of Plutonium-238 Radionuclide Power Sources for Mars-96 International Mission. 2: 8-9.
7. Hiller N, Daniel A, Elsner N, Bass JC, Peyton Moore J (2002) Outgassing and vaporization considerations in milliwatt generators designed for 20-year missions. AIP Conference Proceedings, Space Technology and Applications International Forum-STAIF.
8. Pustovalov AA (1986) Radioisotopic thermoelectric generators for implanted electrocardiostimulant. Atomic Energy: 60, 125-129.
9. UV Lazarenko (1988) Radioisotopic power source for a feeding autonomous apparatus of a type-artificial heart. Atomic Energy: 64, 110-114.
10. Seebeck TJ (1821) Magnetic polarization of metals and minerals. 265: 1822-1823.
11. Goldsmid HJ (1964) Thermoelectric Refrigeration. Plenum Press, New York.
12. Goldsmid HJ (1961) Recent Studies of Bismuth Telluride and Its Alloys. J Appl Phys 32: 2198-2202.
13. Yang B, Wang P (2013) Thermoelectric Microcoolers. 1st Edition, World Scientific Publishing Company, Singapore.
14. Peltier JC (1834) "Nouvelles Experiences sur la caloricite des courans electrique". Ann Chim 371.
15. Thomson W (1851) On a mechanical theory of thermoelectric currents. Edinburgh 91-98.
16. Thomson W (1882) Mathematical Physical Papers. Cambridge Press.
17. Hicks LD, Dresselhaus MS (1993) "Effect of quantum-well structures on the thermoelectric figure of merit". Physical Review B 47.
18. Hicks LD, Harman TC, Dresselhaus MS (1993) "Use of quantum-well superlattices to obtain a high figure of merit from nonconventional thermoelectric materials". Applied Physics Letters 63: 3230-3232.
19. Hicks LD, Dresselhaus MS (1993) "Thermoelectric figure of merit of a one-dimensional conductor". Physical Review B 47: 16631 LP - 16634.
20. Hicks LD, Harman TC, Dresselhaus MS (1993) "Use of quantum-well superlattices to obtain high figure of merit form nonconventional thermoelectric materials". Applied Physics Letters 63: 3230-3232.
21. Dresselhaus MS, Dresselhaus G, Sun X, Zhang Z, Cronin SB, et al, (1999) "The promise of low-dimensional thermoelectric materials". Microscale Thermophysical Engineering 3: 89 - 100.
22. Rowe DM, Min G (1996) "Design theory of thermoelectric modules for electrical power generation". Science, Measurement and Technology, IEE Proceedings 143: 351-356.
23. Sales BC, Mandrus D, Williams RK (1996) "Filled skutterudite antimonides: a new class of thermoelectric materials". Science 272: 1325-1328.
24. Lee SM (1997) "Thermal conductivity of Si Ge superlattices". Applied Physics Letters 70: 2957-2959.
25. Borca-Tasciuc T (1999) "Thermal conductivity of Si/Ge superlattices," in Thermoelectrics. Eighteenth International Conference on 201-204.
26. Venkatasubramanian R (2000) "Lattice thermal conductivity reduction and phonon localizationlike behavior in superlattice structures". Physical Review B 61: 3091-3097.
27. Lin YM (2000) "Theoretical investigation of thermoelectric transport properties of cylindrical Bi nanowires". Physical Review B 62: 4610 LP.
28. Yang B, Chen G (2000) "Lattice dynamics study of phonon heat conduction in quantum wells". Physics of Low-Dimensional Structures 37-48.
29. Heremans J, Thrush C, Lin Y, Cronin S, Zhang Z et al. (2000) "Bismuth nanowire arrays: Synthesis and galvanomagnetic properties". Physical Review B 61: 2921.
30. Chung DY, Hogan T, Brazis P, Rocci-Lane M, Kannewurf C, et al, (2000) "CsBi4Te6: A High-Performance Thermoelectric Material for Low-Temperature Applications". Science 287: 1024-1027.
31. Rabina O, Yu-Ming L, Dresselhaus MS (2001) "Anomalously high thermoelectric figure of merit in Bi1- xSbx nanowires by carrier pocket alignment". Applied Physics Letters 79: 81-83.
32. Venkatasubramanian R, Edward S, Thomas C, Brooks O'Q (2001) "Thin-film

thermoelectric devices with high room-temperature figures of merit". Nature 413: 597-602.

33. Yang B, Chen G (2001) "Lattice dynamics study of anisotropic heat conduction in superlattices". Microscale Thermophysical Engineering 5: 107-116.
34. Harman TC, Taylor PJ, Walsh MP, LaForge BE (2002) "Quantum Dot Superlattice Thermoelectric Materials and Devices". Science 297: 2229-2232.
35. Yang B, Liu JL, Wang KL, Chen G (2002) "Simultaneous measurements of Seebeck coefficient and thermal conductivity across superlattice," Applied Physics Letters 80.
36. Yang B, Liu WL, Liu JL, Wang KL, Chen G (2002) "Measurements of anisotropic thermoelectric properties in superlattices," Applied Physics Letters 81: 3588-3590.
37. Yang B, Chen G (2003) "Partially coherent phonon heat conduction in superlattices". Physical Review B (Condensed Matter and Materials Physics) 67: 195311.
38. Majumdar A (2004) "Materials science: Enhanced: Thermoelectricity in Semiconductor Nanostructures". Science 303: 777-778.
39. Hsu KF (2004) "Cubic $AgPb_m$ $SbTe_{2+m}$: Bulk Thermoelectric Materials with High Figure of Merit". Science 303: 818-821.
40. Yang B, Chen G (2005) "Thermal Conductivity: Theory, Properties and Applications," TM Tritt Ed Kluwar Press 167-186.
41. Nolas GS (2006) "Recent Developments in Bulk Thermoelectric Materials," MRS Bulletin 31: 199-205.
42. Poudel B, Qing H, Yi M, Yucheng L, Austin M (2008) "High-thermoelectric performance of nanostructured bismuth antimony telluride bulk alloys" Science 320: 634-638.
43. Chen G, Dresselhaus MS, Dresselhaus G, Fleurial JP, Caillat T (2003) "Recent developments in thermoelectric materials," International Materials ReviewsS 48: 45-66.
44. Rowe DM (1995) CRC Handbook of Thermoelectrics. Boca Raton: CRC Press.
45. Joshi G, Hohyun L, Yucheng L, Xiaowei W, Gaohua Z (2008) "Enhanced Thermoelectric Figure-of-Merit in Nanostructured p-type Silicon Germanium Bulk Alloys". Nano Letters 8: 4670-4674.
46. Minnich AJ, Dresselhaus MS, Ren ZF, Chen G (2009) "Bulk nanostructured thermoelectric materials: current research and future prospects". Energy & Environmental Science 2: 466-479.
47. Lan Y, Austin Jerome M, Gang C, Zhifeng R (2010) "Enhancement of Thermoelectric Figure-of-Merit by a Bulk Nanostructuring Approach," Advanced Functional Materials 20: 357-376.
48. ASTM (2004) Standard Test Method for Steady-State Heat Flux Measurements and Thermal Transmission Properties by Means of the Guarded-Hot-Plate Apparatus. C177-04 ASTM International.